Acta Crystallographica Section B
Structural Science
ISSN 0108-7681

Predicted crystal structures of tetramethylsilane and tetramethylgermane and an experimental low-temperature structure of tetramethylsilane

Alexandra K. Wolf, Jürgen Glinnemann, Lothar Fink, Edith Alig, Michael Bolte and Martin U. Schmidt*

Goethe University, Institute of Inorganic and Analytical Chemistry, Max-von-Laue-Strasse 7, 60438 Frankfurt am Main, Germany

Correspondence e-mail: m.schmidt@chemie.uni-frankfurt.de

Received 15 December 2009
Accepted 27 January 2010

No crystal structure at ambient pressure is known for tetramethylsilane, $Si(CH_3)_4$, which is used as a standard in NMR spectroscopy. Possible crystal structures were predicted by global lattice-energy minimizations using force-field methods. The lowest-energy structure corresponds to the high-pressure room-temperature phase ($Pa\overline{3}$, $Z = 8$). Low-temperature crystallization at 100 K resulted in a single crystal, and its crystal structure has been determined. The structure corresponds to the predicted structure with the second lowest energy rank. In X-ray powder analyses this is the only observed phase between 80 and 159 K. For tetramethylgermane, $Ge(CH_3)_4$, no experimental crystal structure is known. Global lattice-energy minimizations resulted in 47 possible crystal structures within an energy range of 5 kJ mol^{-1}. The lowest-energy structure was found in $Pa\overline{3}$, $Z = 8$.

1. Introduction

Liquid tetramethylsilane (TMS), $Si(CH_3)_4$ (m.p. 178 K, b.p. 299 K), is widely used as a standard for calibrating chemical shifts in ^{1}H, ^{13}C and ^{29}Si NMR spectroscopy (Hoffman, 2006). Astonishingly, for TMS only a high-pressure crystal structure in $Pa\overline{3}$, $Z = 8$, at 0.58 GPa, 296 K, has been reported so far (Gajda & Katrusiak, 2008). In this structure the molecules are situated on the threefold axes. The symmetry of the molecule is reduced to 3, *i.e.* C_3 (Gajda & Katrusiak, 2008).

According to differential thermal analysis (DTA) TMS forms three polymorphs (Hasebe *et al.*, 1975). The α phase exists from the melting point down to 159 K and seems to be a plastic phase. Upon further cooling the β phase occurs and is stable to 20 K. When the sample is subsequently heated from 20 to 118 K the γ phase is formed. The phases were only identified by DTA, not by X-ray diffraction.

Electron diffraction investigations in the gas phase (Brockway & Jenkins, 1936; Sheehan & Schomaker, 1952; Beagley *et al.*, 1971; Campanelli *et al.*, 2000) and *ab initio* molecular-orbital (MO) calculations (Campanelli *et al.*, 2000) revealed full tetrahedral symmetry, $\overline{4}3m$ (T_d), for the TMS molecule with staggered methyl groups. However, a distortion to symmetry 23 (T) is calculated to be possible. Only one signal is observed in ^{1}H and ^{13}C NMR spectra of liquid TMS, which indicates that all H atoms are equivalent symmetrically. Although TMS is widely used in liquid NMR, no solid-state NMR investigation for TMS has so far been published to the best of our knowledge.

For $Ge(CH_3)_4$ (TMGe, m.p. 185 K, b.p. 316 K) no crystal structure investigations have been reported and only one modification was observed in the temperature range 15–300 K

Table 1
Calculated low-energy crystal structures for TMS by lattice-energy minimizations.

Rank	Energy (kJ mol^{-1})	Space group	Z	Site symmetry of molecule	a (Å)	b (Å)	c (Å)	α (°)	β (°)	γ (°)	V/Z (Å^{-3})
1	−87.920	$Pa\bar{3}$	8	3	11.005	–	–	–	–	–	166.61
2	−86.725	*Pnma*	4	*m*	12.972	8.374	6.278	–	–	–	170.48
3	−86.442	$P2_1/c$	4	1	8.880	9.440	8.203	–	84.32	–	171.05
4	−86.292	$P2_1/m$	2	*m*	6.265	8.388	6.573	–	97.59	–	171.19
5	−86.133	$P\bar{1}$	2	1	6.089	6.311	9.570	89.10	87.80	68.21	170.62
6	−85.920	$P2_1/c$	4	1	7.034	6.745	14.385	–	91.95	–	170.52
7	−85.839	*Pbca*	8	1	11.517	11.071	10.692	–	–	–	170.42
8	−85.743	$P2_1/c$	4	1	12.800	8.961	12.946	–	152.58	–	170.78
9	−85.632	$P2_1/c$	4	1	11.475	10.219	12.389	–	151.95	–	170.79
10	−85.489	$P2_1/c$	4	1	10.697	6.262	13.112	–	128.17	–	172.64
11	−85.488	$P2_12_12_1$	4	1	14.119	6.839	7.083	–	–	–	170.97
12	−85.480	$P\bar{1}$	2	1	5.993	6.322	9.987	87.02	81.63	66.95	172.23
13	−85.437	$P2_1/c$	4	1	11.809	9.332	12.250	–	149.45	–	171.53
14	−85.306	$P2_12_12_1$	4	1	10.563	6.209	10.563	–	–	–	173.19
15	−85.226	$P2_1/c$	4	1	5.885	5.905	19.774	–	94.14	–	171.37
16	−85.195	$P2_1/c$	4	1	10.356	10.753	11.641	–	148.00	–	171.75
17	−85.052	$P2_1/c$	4	1	6.644	6.244	16.745	–	90.58	–	173.64
18	−84.891	*C*2	4	1	10.242	6.906	9.817	–	96.54	–	172.48
19	−84.871	*Pnma*	4	*m*	13.212	8.429	6.235	–	–	–	173.58
20	−84.865	*Ama*2	4	*m*	8.591	10.823	7.500	–	–	–	174.34
21	−84.808	$P2_1/c$	4	1	10.239	6.691	10.355	–	102.02	–	173.45
22	−84.789	*Cmcm*	4	*m*2*m*	7.525	10.902	8.521	–	–	–	174.76
23	−84.763	*Pnma*	4	*m*	7.455	9.523	9.826	–	–	–	174.39
24	−84.592	$P2_1/m$	2	*m*	6.568	8.546	6.666	–	111.06	–	174.57
25	−84.592	*Ama*2	4	*m*	9.742	10.206	7.000	–	–	–	173.99
26	−84.541	$Pmn2_1$	2	*m*	8.351	6.653	6.317	–	–	–	175.50
27	−84.522	$P2_1/m$	4, $Z' = 2$	*m*	6.570	8.479	12.744	–	100.47	–	174.53
28	−84.473	*Aba*2	8	1	19.034	10.085	7.249	–	–	–	173.93
29	−84.451	*R*3*m*	3	3*m*	9.830	–	6.278	–	–	120	175.11
30	−84.445	$P2_1/c$	4	1	10.556	11.477	10.926	–	148.14	–	174.69
31	−84.416	$P2_1/c$	4	1	6.434	17.685	7.994	–	129.72	–	174.90
32	−84.271	$P\bar{1}$	2	1	10.140	6.186	5.886	75.42	78.14	88.18	174.82
33	−84.257	$P2_1/c$	4	1	5.885	18.308	6.786	–	109.72	–	172.06
34	−84.025	$P2_1/c$	4	1	10.771	5.803	11.052	–	90.37	–	172.69
35	−84.009	$P2_1/c$	4	1	6.761	7.561	13.580	–	90.00	–	173.56
36	−83.855	*Pbca*	8	1	19.495	10.372	6.948	–	–	–	175.61
37	−83.720	*Pbca*	8	1	18.390	9.575	8.042	–	–	–	177.00
38	−83.697	*Pnma*	4	*m*	11.153	8.690	7.309	–	–	–	177.10
39	−83.674	*Pbca*	8	1	5.760	11.157	21.559	–	–	–	173.19
40	−83.573	*Pbca*	8	1	5.792	11.322	21.450	–	–	–	175.83
41	−83.456	$P2_1/c$	4	1	9.855	10.461	11.942	–	145.35	–	175.01
42	−83.257	*Pbcm*	4	*m*	6.541	10.510	10.338	–	–	–	177.68
43	−83.254	$P2_1/m$	4, $Z' = 2$	*m*	6.547	10.333	10.508	–	90.99	–	177.69
44	−83.221	*Cc*	4	1	5.842	12.292	10.549	–	111.77	–	175.88
45	−83.125	$Pna2_1$	4	1	10.736	11.187	5.920	–	–	–	177.74

(Valerga & Kilpatrick, 1969). The higher homologous $Sn(CH_3)_4$ and $Pb(CH_3)_4$ each crystallize in the cubic space group $Pa\bar{3}$ with $Z = 8$, with the molecules on threefold axes (Krebs *et al.*, 1989; Fleischer *et al.*, 2003). For neopentane, $C(CH_3)_4$, a cubic modification at 223 K and a tetragonal modification at 123 K could be found (Mones & Post, 1952).

Tetrahalides of Si, SiX_4, with halogen atoms having a comparable size to a methyl group (X = Cl, Br) crystallize either in $P2_1/c$, $Z = 4$ ($SiCl_4$, β-$SiBr_4$) or $Pa\bar{3}$, $Z = 8$ (α-$SiBr_4$; Zakharov *et al.*, 1986; Wolf *et al.*, 2009).

For $Si(CH_3)_3Cl$ two polymorphs could be found: at 157 K the α phase crystallizes in $P2_1/m$ with $Z = 2$; at 0.23 GPa the β phase in $Pmn2_1$ ($Z = 2$) exists (Buschmann *et al.*, 2000; Gajda *et al.*, 2006). Also for the larger derivatives $C[Si(CH_3)_3]_4$ and $Si[Si(CH_3)_3]_4$ several polymorphs could be determined (Dinnebier *et al.*, 1999; Klinkhammer *et al.*, 1995). For $C[Si(CH_3)_3]_4$ three polymorphs are known: below 225 K the compound crystallizes in the cubic space group $P2_13$ with $Z = 4$, between 225 and 268 K in $Pa\bar{3}$, $Z = 4$, and above 268 K a structure in $Fm\bar{3}m$ with $Z = 4$ could be found. For $Si[Si(CH_3)_3]_4$ two polymorphs were described: the high-temperature phase (T = 295 K) crystallizes in $Fm\bar{3}m$ with $Z = 4$; the low-temperature phase (T = 200 K) in $P2_13$ with $Z = 4$. In $Fm\bar{3}m$, $Z = 4$, and $Pa\bar{3}$, $Z = 4$, the structures are disordered. For both compounds lattice-energy calculations were performed (Dinnebier *et al.*, 1999).

In this work we present a full crystal-structure prediction of TMS and TMGe by lattice-energy minimizations. The crystal structure of TMS at 100 K could be determined by low-temperature X-ray single-crystal diffraction. The polymorphism of TMS was investigated by differential thermal analysis and variable-temperature X-ray powder diffraction.

Table 2
Calculated low-energy crystal structures for TMGe by lattice-energy minimizations.

Rank	Energy (kJ mol^{-1})	Space group	Z	Site symmetry of molecule	a (Å)	b (Å)	c (Å)	α (°)	β (°)	γ (°)	V/Z (Å^{-3})
1	−82.565	$Pa\bar{3}$	8	3	11.132	–	–	–	–	–	172.45
2	−81.344	*Pnma*	4	*m*	13.198	8.412	6.346	–	–	–	176.14
3	−81.264	$P2_1/c$	4	1	9.050	9.572	8.200	–	96.02	–	176.59
4	−81.025	$P2_1/m$	2	*m*	6.255	6.721	8.406	–	85.30	–	176.10
5	−80.676	*Pbca*	8	1	11.663	11.241	10.736	–	–	–	175.93
6	−80.423	$P2_1/c$	4	1	10.686	6.326	13.350	–	128.14	–	177.43
7	−80.394	$P2_1/c$	4	1	7.181	6.822	14.413	–	91.80	–	176.44
8	−80.377	$C2/c$	8	1	20.049	6.123	11.624	–	90.23	–	178.36
9	−80.207	$P2_12_12_1$	4	1	6.939	7.193	14.160	–	–	–	176.69
10	−80.132	$P\bar{1}$	2	1	6.223	6.378	9.661	89.16	92.14	111.93	177.75
11	−80.069	*Pnma*	4	*m*	13.419	8.408	6.303	–	–	–	177.78
12	−79.970	$P2_1/c$	4	1	6.759	6.303	16.766	–	90.63	–	178.58
13	−79.901	$P2_1/c$	4	1	5.917	10.438	12.548	–	114.03	–	176.95
14	−79.895	$P2_1/c$	4	1	6.184	9.002	13.198	–	104.80	–	177.59
15	−79.817	$P2_1/c$	4	1	6.430	9.452	12.408	–	109.55	–	177.65
16	−79.770	$P2_1/c$	4	1	6.355	10.820	12.594	–	124.85	–	177.66
17	−79.586	$P2_1/m$	4, $Z' = 2$	*m*	6.693	8.459	12.870	–	100.18	–	179.28
18	−79.563	*Ama*2	4	*m*	8.521	11.021	7.665	–	–	–	179.95
19	−79.563	*Cmcm*	4	*m*2*m*	7.679	11.037	8.497	–	–	–	180.03
20	−79.457	$P\bar{1}$	2	1	5.882	6.788	10.110	81.71	77.15	64.84	177.82
21	−79.431	$P2_1/c$	4	1	10.206	6.827	10.418	–	101.06	–	178.09
22	−79.394	$P2_12_12_1$	4	1	6.361	10.674	10.626	–	–	–	180.37
23	−79.382	$P\bar{1}$	2	1	6.068	6.418	10.142	87.57	81.47	66.88	179.60
24	−79.277	$P2_1/c$	4	1	5.930	5.963	20.139	–	95.22	–	177.29
25	−79.171	$P2_1/c$	4	1	9.640	9.553	8.182	–	75.74	–	182.58
26	−79.112	*Pnma*	4	*m*	7.449	9.713	9.992	–	–	–	180.73
27	−79.106	$P2_1/c$	4	1	10.885	5.849	11.139	–	90.33	–	177.31
28	−79.091	*Pbcn*	4	2	5.852	11.149	10.876	–	–	–	177.41
29	−79.049	$P2_1/c$	4	1	6.934	11.228	10.621	–	120.13	–	178.80
30	−79.025	$P2_1/c$	4	1	7.358	9.327	12.568	–	123.63	–	179.54
31	−79.003	$P2_1/c$	4	1	6.448	10.306	11.886	–	113.44	–	181.17
32	−78.991	$P\bar{1}$	2	1	5.894	6.260	10.156	92.20	102.35	101.49	178.71
33	−78.981	$Pmn2_1$	2	*m*	8.397	6.774	6.384	–	–	–	181.58
34	−78.941	$P\bar{1}$	4, $Z' = 2$	1	5.974	19.196	6.787	87.55	113.63	92.66	178.00
35	−78.911	$P2_1/c$	4	1	6.114	19.846	7.086	–	122.90	–	180.48
36	−78.767	$P\bar{1}$	2	1	5.971	6.507	10.711	87.42	71.36	66.00	179.25
37	−78.767	$P2_1/c$	4	1	5.964	18.348	6.860	–	107.82	–	178.66
38	−78.654	$P2_1/c$	4	1	6.775	7.649	13.832	90.02	–	–	179.20
39	−78.610	$P2_1/c$	4	1	5.993	11.581	11.124	–	110.56	–	180.70
40	−78.601	$P\bar{1}$	4, $Z' = 2$	1	6.870	10.718	12.456	92.10	128.66	92.67	178.24
41	−78.390	*Pnma*	4	*m*	11.308	8.648	7.473	–	–	–	182.69
42	−78.268	*R*3*m*	3	*m*	9.998	–	6.336	–	–	120	182.83
43	−78.256	$P2_1/c$	4	1	5.951	10.987	11.951	–	111.01	–	182.35
44	−78.067	$P2_1/c$	4	1	6.496	17.905	7.886	–	126.85	–	183.50
45	−78.035	$P2_1/c$	4	1	11.293	6.304	11.496	–	117.57	–	181.37
46	−77.884	$P\bar{1}$	2	1	6.780	6.827	8.442	70.74	89.36	82.92	182.94
47	−77.832	$P2_1/c$	4	1	6.797	8.397	12.905	–	82.39	–	182.50

2. Prediction of crystal structures

2.1. Computations

Possible crystal structures of TMS and TMGe were predicted by global minimization of the lattice energy using the program *CRYSCA* (Schmidt & Kalkhof, 1997) and the Dreiding 2.21 force field (Mayo *et al.*, 1990).

In order to check for the applicability of the chosen force-field, lattice-energy test calculations were made on $Sn(CH_3)_4$ and $Pb(CH_3)_4$ for which crystal structures are known. The Dreiding 2.21 force field was developed for atoms carrying Gasteiger charges, but the applied Gasteiger method (Accelrys Ltd, 2003) gave no reliable results for TMS, TMGe, TMSn and TMPb. To obtain more suitable charges, quantum-chemical *ab initio* calculations were performed for all $E(CH_3)_4$ molecules (E = C, Si, Ge, Sn, Pb) using the SDD basis set (Igel-Mann *et al.*, 1988; Küchle *et al.*, 1991; Bergner *et al.*, 1993) in the *GAUSSIAN* program package (Frisch *et al.*, 2003). For $C(CH_3)_4$ the resulting Mullikan charges were 7.6 times higher than the Gasteiger charges; correspondingly, the Mullikan charges for TMS, TMGe, TMSn and TMPb were scaled by 7.6^{-1}.

In the test calculations on $Sn(CH_3)_4$ and $Pb(CH_3)_4$ the lowest-energy structures correspond to the experimental structures (both $Pa\bar{3}$, $Z = 8$) with high accuracy. This indicates the applicability for the Dreiding 2.21 force field for this class of compound.

The molecular geometry of TMS and TMGe was set up manually. The Si—C bond length of 1.877 Å was taken from electron-diffraction data (Campanelli *et al.*, 2000). The Ge—C bond length of 1.970 Å was set according to the Dreiding 2.21 force field. To account for the molecular flexibility of TMS, a

Table 3
Crystallographic data for TMS at 100 K.

Crystal data	
Chemical formula	$C_4H_{12}Si$
M_r	88.23
Crystal system, space group	Orthorhombic, *Pnma* (62)
Temperature (K)	100
a, *b*, *c* (Å)	13.131 (3), 8.198 (3), 6.3290 (10)
V (Å^3)	681.3 (3)
Z	4
Radiation type	Mo *Kα*
μ (mm^{-1})	0.21
Crystal size (mm^3)	0.40 × 0.40 × 0.40
Data collection	
Diffractometer	STOE IPDS II two-circle
Absorption correction	Multi-scan *MULABS* (Spek, 2003; Blessing, 1995)
T_{min}, T_{max}	0.920, 0.920
No. of measured, independent and observed [$I > 2\sigma(I)$] reflections	1818, 635, 466
R_{int}	0.143
Refinement	
$R[F^2>2\sigma(F^2)]$, $wR(F^2)$, *S*	0.123,† 0.335,† 1.21
No. of reflections	635
No. of parameters	28
No. of restraints	0
H-atom treatment	H-atom parameters constrained
$\Delta\rho_{max}$, $\Delta\rho_{min}$ (e Å^{-3})	0.61, −0.69

† The relatively high *R* values arise from the experimental procedure to obtain the crystal. As described in §3.3, the compound was filled in a glass capillary and shock cooled to *T* = 100 K. The quality of the data suffered from the crystal being in a capillary surrounded by non-crystalline material.

potential for the rotation of the methyl groups was included. This potential was fitted on MP2/6–311+G(d,p) calculations. In the lattice-energy calculations no significant rotation of the methyl group was observed in any calculated crystal structure of TMS; hence the orientation of the methyl group was fixed to staggered in the *CRYSCA* calculations of TMGe.

The lattice-energy calculations were performed in statistically frequent space groups for molecular compounds ($P\overline{1}$, $Z = 2$; $P2_1$, $Z = 2$; Cc, $Z = 4$; $P2_1/c$, $Z = 4$; $P2_12_12_1$, $Z = 4$; $Pna2_1$, $Z = 4$; $Pca2_1$, $Z = 4$; $Pbca$, $Z = 8$ and $P1$, $Z = 1$; each with $Z' = 1$). Since the molecule itself is highly symmetrical, various supergroups could be reached. For example, $C2/c$ ($Z = 4$) with molecules on twofold axes can be reached from Cc ($Z = 4$) or $P2_1/c$ ($Z = 4$); $Pbcn$ ($Z = 4$) can result from $P2_1/c$, $Pna2_1$ or $Pca2_1$ (each with $Z = 4$); $Pa\overline{3}$ ($Z = 8$, molecules on threefold axes) can be formed during calculations in the subgroup $Pbca$ ($Z = 8$); and $I\overline{4}2m$ ($Z = 2$) can be reached from a calculation in $P1$ ($Z = 1$) or $P2_1$ ($Z = 2$).

The minimizations started from a set of 10 000 different structures for each space group with random starting values for the lattice parameters, the position and the orientation of the molecule, and for the torsion angles of the four methyl groups of TMS.

All low-energy structures (excluding duplicates) were post-optimized using the Dreiding 2.21 force field for intermolecular interactions to account for all the packing effects (*i.e.* the deformation of the molecule by packing forces). During the calculations with the programm package *Cerius*^{2} (Accelrys Inc., 2003) the geometry of the molecule was optimized simultaneously with its position and orientation, and with the lattice parameters. All structures were inspected for higher symmetry, and if necessary, transformed to the corresponding supergroups. The resulting space groups do not have to be consistent with the starting space groups because for the post-optimization all structures were set to the space group *P*1. A further post-optimization of the transformed structures showed no significant changes in energy or structure in any case. As a verification several structures were post-optimized using the program package *Materials Studio* (Accelrys Inc., 2008) resulting in exactly the same structures as the optimization with the program package *Cerius*^{2}.

2.2. Results for TMS

In an energy range of 5 kJ mol^{-1} 45 low-energy crystal structures were found (Table 1). These may be considered as potential polymorphs. All structures were found several times from different starting points, indicating that the calculations were complete and no low-energy structure is missing. The energetically best crystal structure was found in $Pa\overline{3}$, $Z = 8$, with the molecules on threefold axes. The energetically second best structure shows symmetry *Pnma*, $Z = 4$, with the molecules on the mirror planes. It is $\sim$ 1.2 kJ mol^{-1} less favorable than the energetically best structure.

2.3. Results for TTMGe

For tetramethylgermane 47 low-energy crystal structures were found in the energy range 5 kJ mol^{-1} (Table 2). Just as for tetramethylsilane the energetically best crystal structure was found in $Pa\overline{3}$, $Z = 8$, with the molecules on threefold axes and the energetically second best structure in *Pnma*, $Z = 4$, with the molecules on the mirror planes.

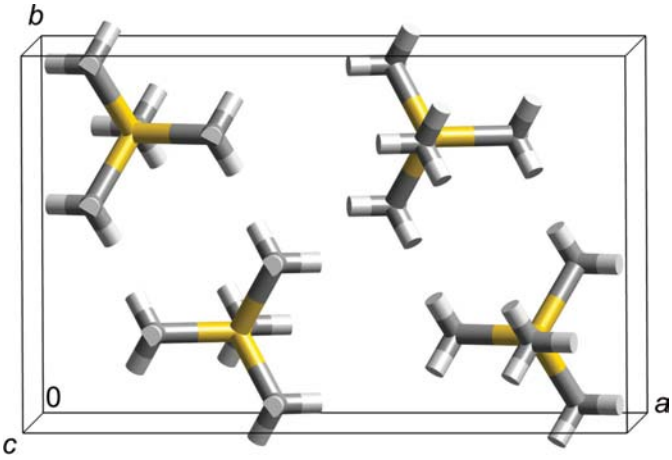

Figure 1
Experimental structure of TMS at *T* = 100 K in *Pnma*, *Z* = 4.

Table 4
Predicted and experimental crystallographic data of TMS.

Pnma, $Z = 4$	Experimental, T = 100 K, p = 1013.25 hPa	Calculated	Difference (%)
a (Å)	13.131 (3)	12.972	−1.21
b (Å)	8.198 (3)	8.374	2.15
c (Å)	6.3290 (10)	6.278	−0.81
V (Å^3)	681.3 (3)	681.9	0.09
Si−C1 (Å)	1.861 (9)	1.875	0.75
Si−C2 (Å)	1.864 (7)	1.875	0.59
Si−C3 ×2 (Å)	1.874 (6)	1.876	0.11

$Pa\bar{3}$, $Z = 8$	Experimental, T = 296 K, p = 0.95 GPa	Calculated	Difference (%)
a (Å)	10.7328 (13)	11.005	2.54
V (Å^3)	1236.3 (3)	1332.9	7.81
Si−C1 ×2 (Å)	1.850 (11)	1.876	1.41
Si−C2 ×2 (Å)	1.855 (5)	1.876	1.13

3. Experimental investigations of a low-temperature crystal structure of TMS

3.1. Thermal analysis

Differential thermal analysis was performed between 110 and 293 K on a SETARAM TG/DTA with a cooling rate of 5 K min^{-1}. The sample was cooled down from 293 to 110 K and subsequently heated to 293 K. The thermogram is in agreement with previous studies (Hasebe *et al.*, 1975). Upon cooling an irreversible phase transition at 159 K could be determined. No indication of a transition to the γ phase could ever be observed. Obviously the γ phase is only obtained when cooled to lower than 110 K.

3.2. X-ray powder diffraction

Powder diffraction of TMS was performed with Cu $K\alpha_1$ radiation ($\lambda = 1.5406$ Å) using a Stoe Stadi-P diffractometer in transmission mode. The sample was placed in a glass capillary with 1.0 mm diameter and rotated during the measurements. Measurements were carried out at lower temperatures (80–160 K).

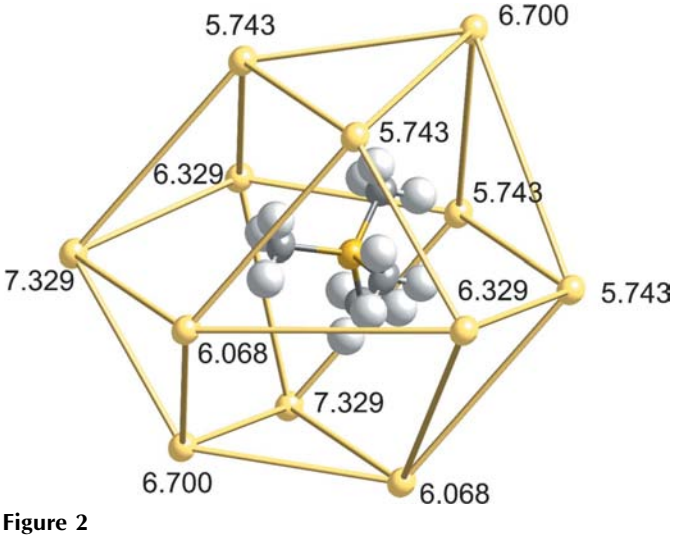

Figure 2
The coordination of TMS at $T = 100$ K in *Pnma*, $Z = 4$. Only the Si atoms of the neighbouring molecules have been shown. The distances between the central Si atom and the neighbouring Si atoms are given in Å.

3.3. Single-crystal analysis

3.3.1. Experimental. TMS purchased from Merck was used without any purification. TMS was filled in a glass capillary with 1.0 mm diameter. The sample was then shock-cooled to T = 100 K. A single crystal suitable for X-ray structure determination was obtained. The diffraction data were collected at 100 K using a Stoe IPDS-II diffractometer with Mo $K\alpha$ radiation.

The data have been integrated using the *X-Area* program (Stoe & Cie, 2001). An empirical absorption correction has been applied to the data using *SORTAV* (Blessing, 1995), as implemented in *PLATON* (Spek, 2003).

The structure was solved by direct methods using *SHELXS*90 (Sheldrick, 2008) and refined with full-matrix least-squares against F^2 using *SHELXL*97 (Sheldrick, 2008). H atoms were geometrically positioned and refined with fixed individual isotropic displacement parameters [U(H) = 1.5U_{eq}(C)] using a riding model with C−H = 0.98 Å.

3.3.2. Results. At 100 K TMS crystallizes in *Pnma* with $Z = 4$, with the molecules on the mirror planes (Table 3, Fig. 1). The symmetry of the molecule is *m*.

The methyl groups are rotated by less than 1°. Thus the TMS molecule exhibits full tetrahedral symmetry with respect to the experimental errors. Each molecule has 12 neighbours on the corners of a distorted cuboctahedron. The shortest

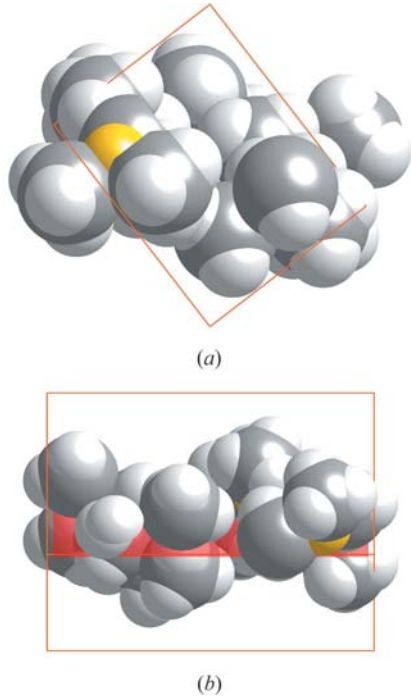

Figure 3
Crystal packing of TMS at 100 K in *Pnma*, $Z = 4$. (*a*) View along [100]. (*b*) View along [0$\bar{1}$2]. The lattice plane (011) is given in red.

distance between two Si atoms is 5.743 Å, the largest 7.329 Å (Fig. 2).

The structure forms layers along (011) (Fig. 3).

4. Discussion

For TMS the two predicted energetically best structures could be verified experimentally. Both predicted structures are very similar to the experimental ones (Table 4, Figs. 4 and 5).

The observed crystal structure at 100 K (*Pnma*, $Z = 4$) corresponds to the predicted structure at rank 2 (Table 1). In the experimental as well as in the calculated structure, the molecules are situated on the mirror planes.

The methyl groups are rotated by less than 1°. For the high-pressure phase a rotation of the methyl groups of 17.5° from the full staggered conformation is described. Other tetrahedral molecules also show distortions from the full staggered conformation in the solid state; for $Si[Si(CH_3)_3]_4$ the trimethylsilyl groups are rotated by 13.7 and 17.5°. In the structure of $C[Si(CH_3)_3]_4$, at 295 K, the trimethylsilyl groups are rotated by 18.8 and 27.5°. For the low-temperature phase of the same compound at 150 K rotations by 20.5 and 14.4° are observed.

Table 5
Structure types for published EX_4 compounds (after Wolf *et al.*, 2008).

Abbreviations for (distorted) structure types: c.c.p. – cubic close packing; h.c.p. – hexagonal close packing; b.c.c. – body-centred cubic packing as in W; c.p. – cubic primitive as in Po; s – like sulfur partial structure in pyrite (FeS_2); 'h.c.p.' – an intergrowth of mainly h.c.p. with c.c.p.

Space group	Z	Site symmetry of molecule	Arrangement of the molecules/arrangement of X atoms
$I\bar{4}3m$	2	$\bar{4}3m$	b.c.c./c.p.
$P\bar{4}3m$	1	$\bar{4}3m$	c.p./c.c.p.
$I\bar{4}2m$	2	$\bar{4}2m$	c.c.p./b.c.c.
$Pa\bar{3}$	8	3	s/c.c.p.
$C2/c$	4	2	c.c.p./c.c.p.
$P2_1/c$	4	1	h.c.p./h.c.p.
$C2/c$	32	all 1	c.c.p./'h.c.p.'

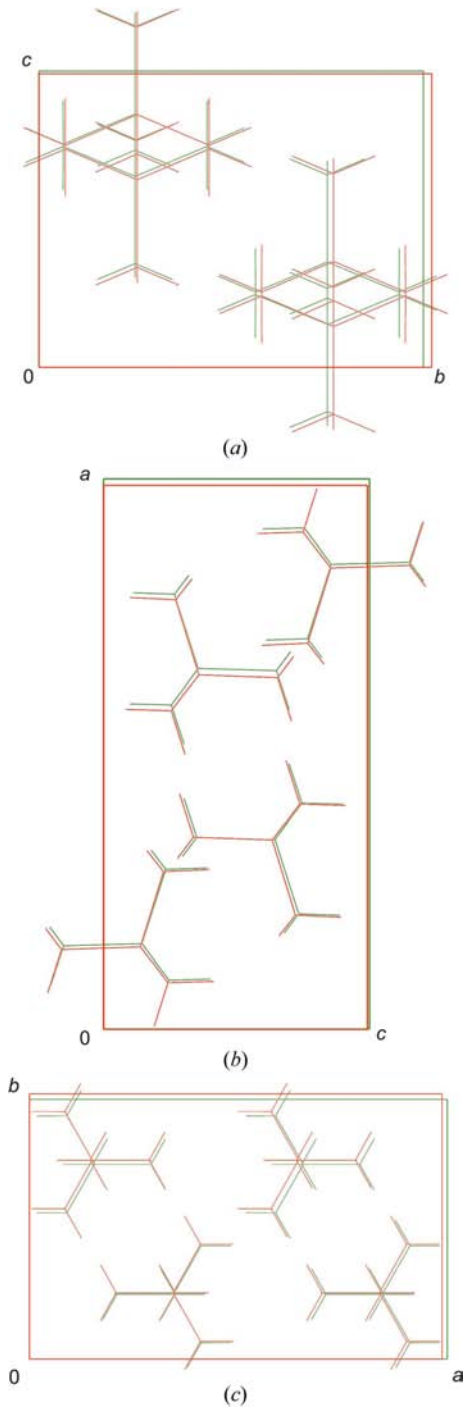

Figure 4
Superposition of the calculated (red) and experimental (green) structures of TMS in *Pnma*, $Z = 4$. (*a*) View along [100]. (*b*) View along [010]. (*c*) View along [001].

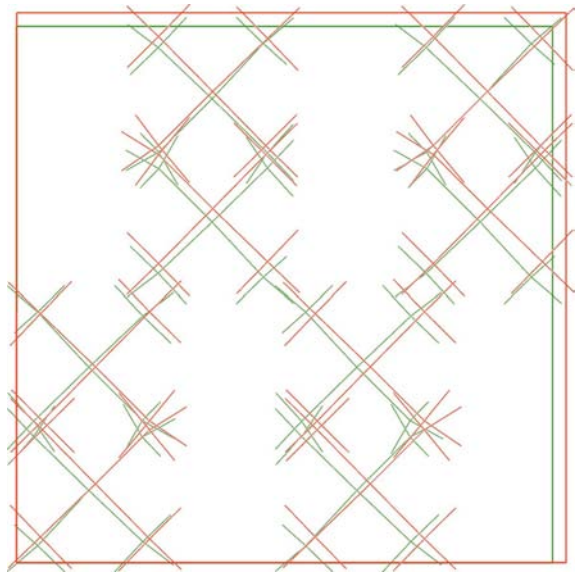

Figure 5
Superposition of the calculated (red) and experimental (green) structures of TMS in $Pa\bar{3}$, $Z = 8$. View along [100].

In the *Pnma* structure of TMS each molecule has 12 neighbours (Fig. 2). In the high-pressure phase of TMS the coordination number increases to 12 + 1 neighbours.

In the crystal structures of EX_4 molecules, where E = C, Si, Ge, Sn, Pb and X = F, Cl, Br, I, the X atoms as well as the molecules themselves tend to form close packings (Table 5; Wolf *et al.*, 2008). In TMS at 100 K the C atoms and thus the methyl groups form a distorted hexagonal close packing (h.c.p.) with the Si atoms occupying 1/8 of the tetrahedral voids. The Si atoms and thus the molecules themselves form a distorted cubic close packing (c.c.p.; Fig. 6). This structure type is a new one (Table 5).

The high-pressure phase at 0.95 GPa, 296 K ($Pa\overline{3}$, $Z = 8$; Gajda & Katrusiak, 2008) corresponds to the predicted structure at rank 1 (Table 1). In the experimental as well as in the calculated structure, the molecules are situated on three-fold axes. The C atoms and thus the methyl groups form a distorted cubic close packing. The Si atoms occupy 1/8 of the tetrahedral voids in such a way that two Si atoms are arranged like the S atoms in pyrite (FeS_2) or the O atoms in solid CO_2 (Mark & Pohland, 1926; Simon & Peters, 1980). This structure type is also found experimentally for SiI_4, $GeBr_4$, SnI_4, $Pb(CH_3)_4$ and $Sn(CH_3)_4$ (Table 5, Fig. 7; Wolf *et al.*, 2008).

For $Ge(CH_3)_4$ possible polymorphs could be predicted by global lattice-energy minimizations. The energetically best crystal structure $Pa\overline{3}$, $Z = 8$ (Fig. 8), is isostructural to the high-pressure phase of TMS and the experimental structures of TMSn and TMPb. The energetically second best structure *Pnma*, $Z = 4$, is ~ 1.221 kJ mol^{-1} less favorable than the energetically best structure, and it is isomorphic to the low-temperature structure of TMS.

5. Conclusion

By global lattice-energy minimizations 45 possible crystal structures for TMS were predicted within an energy range of 5 kJ above the global minimum. The two energetically best structures were verified experimentally from high-pressure single-crystal X-ray diffraction (Gajda & Katrusiak, 2008) and low-temperature single-crystal X-ray diffraction data (this work). The high-pressure phase crystallizes in $Pa\overline{3}$ ($Z = 8$) and the low-temperature phase crystallizes in *Pnma* ($Z = 4$).

Global lattice-energy calculations for TMGe showed that in the energy range 5 kJ mol^{-1} 47 low-energy crystal structures were found. These may be considered as potential polymorphs. The energetically best crystal structure was found in the cubic space group $Pa\overline{3}$, $Z = 8$, with the molecules on

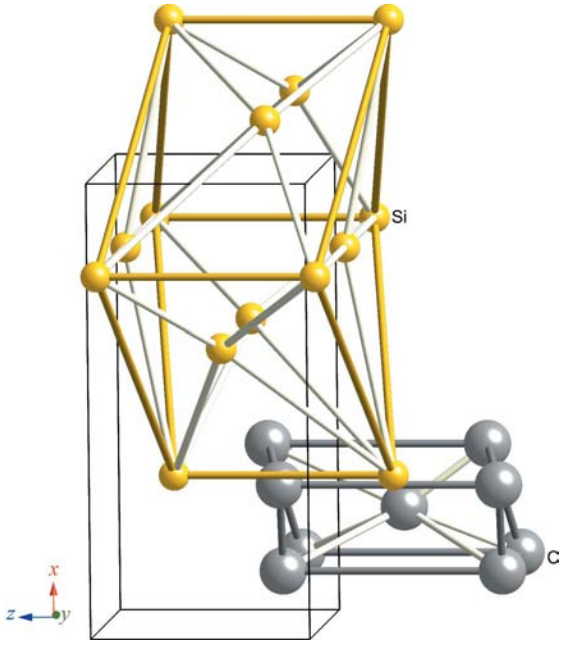

Figure 6
Structure type *Pnma*, $Z = 4$ – c.c.p./h.c.p. Thin black lines: edges of the unit cell of the TMS structure; yellow balls and yellow rods: unit cell of the partial structure of the Si atoms, a distorted c.c.p.; grey balls and grey rods: unit cell of the partial structure of the C atoms, a distorted h.c.p.

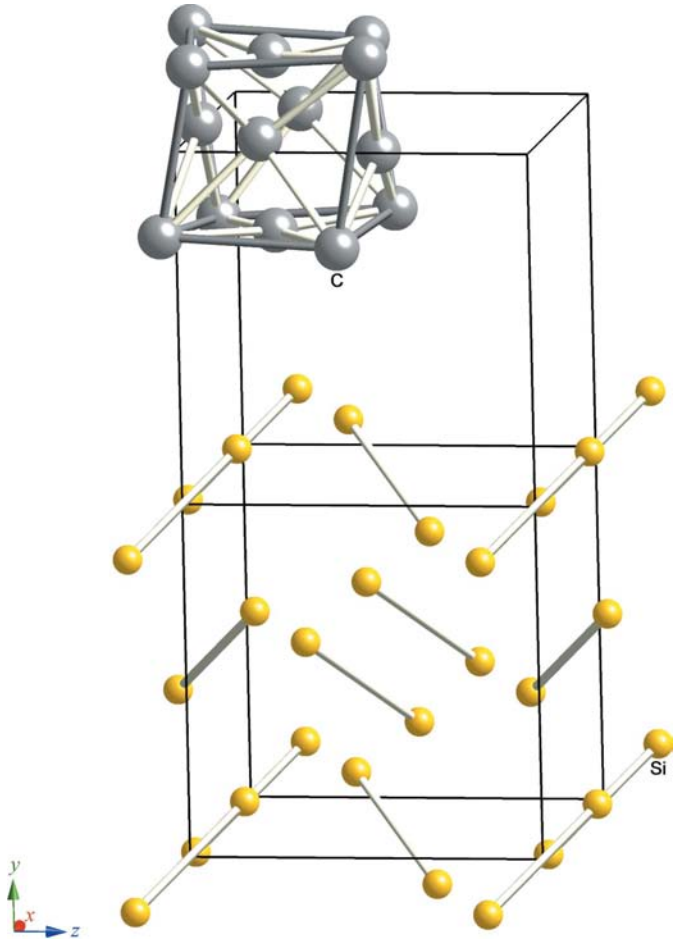

Figure 7
Structure type $Pa\overline{3}$, $Z = 8$ – s/c.c.p. Thin black lines: edges of two unit cells of the TMS structure; yellow balls and light-grey rods: the partial structure of the Si atoms, like the S_2^{2-} dumbbells in the FeS_2 pyrite structure (s); grey balls and grey rods: the partial structure of the C atoms, a distorted c.c.p.

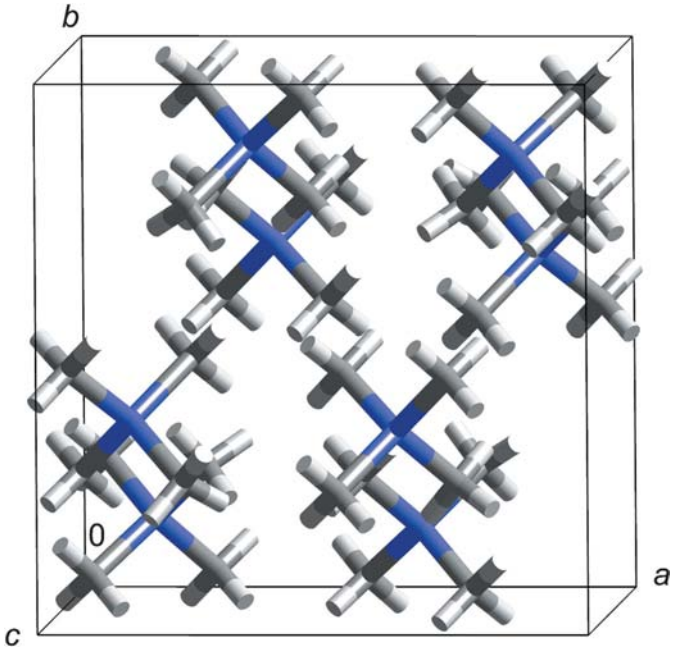

Figure 8
Calculated lowest-energy structure of TMGe in $Pa\bar{3}$, $Z = 8$.

threefold axes. The energetically second best structure *Pnma*, $Z = 4$, is ~ 1.175 kJ mol^{-1} less favorable than the energetically best structure. Both energetically best structures are isostructural to the structures experimentally found for TMS.

References

Accelrys Inc. (2003). *Cerius*^{2}, Version 4.9. Accelrys Inc., San Diego, USA.

Accelrys Inc. (2008). *Materials Studio* 4.4. Accelrys Inc., San Diego, USA.

Beagley, B., Monaghan, J. J. & Hewitt, T. G. (1971). *J. Mol. Struct.* **8**, 401–411.

Bergner, A., Dolg, M., Küchle, W., Stoll, H. & Preuss, H. (1993). *Mol. Phys.* **80**, 1431–1441.

Blessing, R. H. (1995). *Acta Cryst.* A**51**, 33–38.

Brockway, L. O. & Jenkins, H. O. (1936). *J. Am. Chem. Soc.* **58**, 2036–2044.

Buschmann, J., Lentz, D., Luger, P. & Röttger, M. (2000). *Acta Cryst.* C**56**, 121–122.

Campanelli, A. R., Ramondo, F., Domenicano, A. & Hargittai, I. (2000). *Struct. Chem.* **11**, 155–160.

Dinnebier, R. E., Dollase, W. A., Helluy, X., Kümmerlen, J., Sebald, A., Schmidt, M. U., Pagola, S., Stephens, P. W. & van Smaalen, S. (1999). *Acta Cryst.* B**55**, 1014–1029.

Fleischer, H., Parsons, S. & Pulham, C. R. (2003). *Acta Cryst.* E**59**, m11–m13.

Frisch, M. J. *et al.* (2003). *GAUSSIAN*03, Revision B.01. Gaussian Inc., Pittsburgh PA, USA.

Gajda, R., Dziubek, K. & Katrusiak, A. (2006). *Acta Cryst.* B**62**, 86–93.

Gajda, R. & Katrusiak, A. (2008). *Cryst. Growth Des.* **8**, 211–214.

Hasebe, T., Soda, G. & Chihara, H. (1975). *Proc. Jpn Acad.* **51**, 168–172.

Hoffman, R. E. (2006). *Magn. Reson. Chem.* **44**, 606–616.

Igel-Mann, G., Stoll, H. & Preuss, H. (1988). *Mol. Phys.* **65**, 1321–1328.

Klinkhammer, K. W., Kühner, S., Regelmann, B. & Weidlein, J. (1995). *J. Organomet. Chem.* **496**, 241–243.

Krebs, B., Henkel, G. & Dartmann, M. (1989). *Acta Cryst.* C**45**, 1010–1012.

Küchle, W., Dolg, M., Stoll, H. & Preuss, H. (1991). *Mol. Phys.* **74**, 1245–1263.

Mark, H. & Pohland, E. (1926). *Z. Kristallogr.* **64**, 113–114.

Mayo, S. L., Olafson, B. D. & Goddard III, W. A. (1990). *J. Phys. Chem.* **94**, 8897–8909.

Mones, A. H. & Post, B. (1952). *J. Chem. Phys.* **20**, 755–756.

Schmidt, M. U. & Kalkhof, H. (1997). *CRYSCA*. Frankfurt Am Main, Germany.

Sheehan, W. F. & Schomaker, V. (1952). *J. Am. Chem. Soc.* **74**, 3956.

Sheldrick, G. M. (2008). *Acta Cryst.* A**64**, 112–122.

Simon, A. & Peters, K. (1980). *Acta Cryst.* B**36**, 2750–2751.

Spek, A. L. (2003). *J. Appl. Cryst.* **36**, 7–13.

Stoe & Cie (2001). *X-AREA*. Stoe and Cie, Darmstadt, Germany.

Valerga, A. J. & Kilpatrick, J. E. (1969). *J. Chem. Phys.* **52**, 4545–4549.

Wolf, A. K., Glinnemann, J. & Schmidt, M. U. (2008). *CrystEngComm*, **10**, 1364–1371.

Wolf, A. K., Glinnemann, J., Schmidt, M. U., Tong, J., Dinnebier, R. E., Simon, A. & Köhler, J. (2009). *Acta Cryst.* B**65**, 342–349.

Zakharov, L. N., Antipin, M. Y., Struchkov, Y. T., Gusev, A. V., Gibbin, A. M. & Zhernenkov, N. V. (1986). *Kristallografiya*, **31**, 171–172.